CHAPTER 47

MODELING SEDIMENTATION AT INLET AND COASTAL REGION

Pang-Mou Lin,[1] A.M., ASCE
Civil Engineer Assistant
Dept. of County Engineer, County of Los Angeles
California, U.S.A.

ABSTRACT

Sediment transport in the vicinity of inlets and coastal regions depends on the combined bottom shear stresses due to both currents and waves. The modeling of the movement of bedload is controlled by the Froude law, bottom shear stress, wave steepness, and friction factor. Assuming Einstein's theory of bedload function can be applied to this study, an analysis was performed after conducting experiments in the flume and model basin. A series of results obtained from the flume tests is to insure the relationship between the fluid characteristic and the movement of bedload. The final results concerning the longshore sediment transport appeared satisfactory with the estimated curves. The bottom configurations in the inlet after each test were also shown satisfactorily similar. The sedimentological time scale for the three bed materials were not in satisfactory agreement, however, more discussion of the results was presented in this paper.

INTRODUCTION

Problems dealing with sediment transport in the vicinity of inlet and coastal region are very comlex and difficult. Very often, analytical solution fall short because of insufficient knowledge of phenomena, or because of complex geometry. In such cases, a model study with a movable bed is desirable and is a valuable quide to the engineer in the design of coastal structures and navigational channels.

---

1) Former graduate assistant, Dept. of Coastal and Oceanographic Engineering, University of Florida. Gainesville, Florida, U.S.A.

It is desirable to use lighter movable bed material to reduce the operation time of the model. In this research, the similarity of movable beds was studied by using sand, walnut shell, and coal. The characteristics of bed materials is shown below

Material	Spec. Gravity	D_{80}	D_{50}	D_{20} (mm)
Sand	2.67	0.23	0.16	0.14
Walnut shell	1.35	1.60	1.60	1.25
Coal	1.25	0.84	0.76	0.53

The movement of sand along the coast and in the inlet is induced by both currents and waves action. Many investigators have arrived at a relationship between currents and sediment transport (1), and to a lesser extent, between waves and sediment transport (2). The combined action of waves and currents in sediment transport is not completely understood yet. In order to have a better understanding of this problem, a series of tests was conducted in which different materials were used to verify the similarity laws. The test program consisted of (I) a basic investigation of grain movement of different materials in a one-dimensional flume, and (II) a model study of waves and currents in a inlet and a coastal region under consideration similar to the ones found in nature. Separate tests were conducted for inlet currents, waves approaching the coastal line at an angle, and a combination of waves and currents. The acquired measurements consisted of currents in the inlet, wave heights, and longshore sediment transports. After each run, the bottom configuration was contoured and recorded photographically.

THEORETICAL REVIEW

The consideration of modeling velocity parameters in the model basin is shown in Figure 1_a and the respective flow equations are expressed below

EBB FLOW

$$V_x = \frac{V_m}{2C_2} \cdot \frac{B_1}{x} \exp\left(-\frac{1}{2C_2^2} \cdot \frac{y^2}{x^2}\right) \qquad (1)$$

$$V_y = \frac{V_m}{2C_2} \cdot \frac{B_1 \cdot y}{x^2} \exp\left[-\frac{y^2}{2C_2^2 x^2}\right] \tag{2}$$

FLOOD FLOW

$$\cosh^2 \log \frac{V}{q} = \tfrac{1}{2}\left\{(e^{\frac{2\pi\phi}{Q}} + 1) + \left[(e^{\frac{2\pi\phi}{Q}} + 1)^2 - 4e^{\frac{2\pi\phi}{Q}} \sin^2\left(\frac{\pi\psi}{Q}\right)\right]^{\frac{1}{2}}\right\} \tag{3}$$

where $V = \frac{2+\pi}{\pi} V_m$

LONGSHORE CURRENT

$$V_L^2 = \frac{3}{8} \frac{gH_b^2 \cdot n_b}{d_b} \cdot \frac{\sin\alpha \cdot \sin\theta_b \cdot \sin 2\theta_b}{f} \tag{4}$$

where $f = \left[2 \log_{10}\left(\frac{d_b}{k_e}\right) + 1.74\right]^{-2}$

HORIZONTAL ORBITAL VELOCITY

$$u = \frac{H}{2} \frac{\cosh ky}{\sinh kd} \sin(kx - \sigma t) \tag{5}$$

The basic analytical treatment of channel expansion of ebb flow is assumed to be the same as that for a half circular jet expansion. The theory of circular jet expansion was first described in detail by Tollmien (3) and later investigators, for example, Albertson, Dai, Jensen and Rouse (4) and Baines (5). It is resonable to apply this theory in the course of the analysis of ebb flow pattern. Concerning the flood flow pattern,

the basic analytical treatment was presented by French (6) in his research. It is resonable to apply potential flow phenomenon to the flood flow condition. The longshore current is based on Eagleson's experimental result (7). No direct measurement of longshore current velocity was conducted in this study, however, the friction coefficient f was obtained by using the Karman-Prandtl resistance equation for steady uniform flow. The values of absolute roughness height k_e in thepresent study were assumed according to both Eagleson's report and the velocity profiles measured in the flume tests. The average values of roughness height k_e are shown below

Material	k_e (ft.)
Sand	0.0058
Walnut shell	0.00092
Coal	0.00054

It is assumed that the bedload transport, due to the combined action of waves and currents, is a function of bottom shear stress. Apply Prandtl's turbulent shear stress equation

$$\tau = \rho \ell^2 \left(\frac{\partial V(y)}{\partial y} \right)^2 \tag{6}$$

and make the assumption that the velocity profile

$$V(y) = \frac{V_*}{\kappa} \log \frac{y}{k_e} \tag{7}$$

from the edge of the vicous sublayer to the granular surface, is linear. The combined shear stresses are expressed as follows.

Ebb flow inside channel

$$\tau(t) = \rho V_{m_*}^2 \left| 1 - \xi \frac{p_1 u_o}{V_m} \cos\theta \sin\sigma t \right| \left(1 - \xi \frac{p_1 u_o}{V_m} \cos\theta \sin\sigma t\right) \tag{8}$$

Ebb flow parallel to the shoreline

$$\tau(t) = \rho V_{L_*}^2 \left| \frac{V_L - V_y}{V_L} + \xi \frac{p_1 u_o}{V_L} \sin\theta \sin\sigma t \right| \left(\frac{V_L - V_y}{V_L}\right.$$

$$+\xi\frac{p_1 u_o}{V_L}\sin\theta\ \sin\sigma t) \tag{9}$$

Flood flow inside channel

$$\tau(t) = \rho q_*^2 \left| \frac{q_x}{q} + \xi\frac{p_1 u_o}{q}\cos\theta\ \sin\sigma t \right| \left(\frac{q_x}{q} + \xi\frac{p_1 u_o}{q}\cos\theta\ \sin\sigma t\right) \tag{10}$$

Flood flow parallel to the shoreline

$$\tau(t) = \rho V_{L*}^2 \left| \frac{V_L - q_y}{V_L} + \xi\frac{p_1 u_o}{V_L}\sin\theta\ \sin\sigma t \right| \left(\frac{V_L - q_y}{V_L} + \xi\frac{p_1 u_o}{V_L}\sin\theta\ \sin\sigma t\right) \tag{11}$$

where $\xi = \dfrac{C_z \cdot K}{g^{\frac{1}{2}}}$

p_1 is the coefficient of horizontal orbital velocity above the viscous sublayer and was determined experimentally in this study. After integration for a wave period (see appendix I) the shear stress can be expressed in terms of the shear velocity and a dimensionless coefficient η_x as expressed below

$$\tau = \rho V_*^2 \cdot \eta_x \tag{12}$$

where $\eta_x = \dfrac{1}{T}\displaystyle\int_o^T \frac{\tau(t)}{\rho V_*^2}\,dt$

Bagnold (8) found that the bed shear stress τ_c required to

maintain the motion of bedload is shown in the equation

$$\tau = (\rho_s - \rho_f)\, g.d_e.\theta' \qquad (13)$$

where $\theta' = C_o \tan\alpha_1$ a dimensionless shear stress parameter

where C_o is static volume concentration of bed material, α_1 is the internal friction angle of bed material. The magnitude of θ' does affect the intensity of the movement of bed material. Considering the similarity law, θ' is one of the essential parameters to simulate the bed shear stresses between two different bed materials. The dimensionless critical shear stress parameter θ_c for each bed material was obtained from the results of flume tests.

Applying an empirical relationship between shear stress and sediment transport rate by the Einstein's result as shown below

$$\frac{q_s}{F_o.\left[g(S_s - 1)d_e^3\right]^{\frac{1}{2}}} = 40\left(\frac{\tau}{\rho g(S_s - 1)\, d_e}\right)^3 \qquad (14)$$

$$\text{where } F_o = \left[\frac{2}{3} + \frac{36\nu^2}{gd_e^3(S_s - 1)}\right]^{\frac{1}{2}} - \left[\frac{36\nu^2}{gd_e^3(S_s - 1)}\right]^{\frac{1}{2}}$$

and the equation of conservation of sediment mass transport

$$\frac{dy}{dt} + \frac{1}{\rho_w g(S_s - 1)(1 - p)} \frac{dq_w}{dx} = 0 \qquad (15)$$

The time scale of sediment transport is obtained and shown as

$$\lambda_t = \frac{\lambda_{C_z}}{\lambda_V^6} \cdot \lambda_{d_e}^{3/2} \cdot \frac{\lambda_{(S_s - 1)}^{5/2} \cdot \lambda_L^2}{\lambda_{\eta_x}^3 \cdot \lambda_{F_o}} \tag{16}$$

From the above analysis, it is possible to summarize the movable bed parameters by a functional relationship of the form

$$f_1 \left[d_e(S_s - 1)\theta_c, d, V, g, V_*, H, L \right] = 0 \tag{17}$$

The choice of parameters implies that the particle shape and its size distribution, fluid characteristics, wave characteristics, and movement of bedload are significant. Using the Buckingham π - theorm, a functional relationship among four dimensionless parameters is expressed below

$$f_2 \left[\frac{V}{\sqrt{gd}}, \frac{V_*^2}{g(S_s - 1)d_e \cdot \theta_c}, \frac{V}{V_*}, \frac{H}{L} \right] = 0 \tag{18}$$

It is to be noted that velocity scale is determined first from the experimental result of the value of θ_c and C_z, then the depth scale and time scale of wave period are calculated from the undistorted model law.

TEST PROCEDURE AND RESULTS

A schematic diagram of the flume is shown in Figure 1b. The flume is 60 feet long, 3 feet deep, and 2 feet wide and has maxium slope of 2 per cent and a maximum discharge of 5.8 cfs. The tests in the flume were conducted for three types of granular beds. These were made of sand, ground walnut shell, and bituminous coal. Water was allowed to flow until the flow was statistically steady and uniform in the test section. For each bed material, a series of tests was carried out with various combinations of mean depth and flow velocity. Velocity measurements were obtained at different elevations in the test section. A propeller-type velocity meter, manufactured by A. Ott Kempten (Germany), was used for this purpose.

The bed materials were arranged in the middle portion of the flume at a thickness of 2 inches along a 30 foot test section. In order to obtain the velocity profile which produces the critical shear stress, the water discharge was increased slowly in small increments spaced by ten-minute intervals. When the bed material underwent intermittent motion, the velocity profiles were measured at that stage. The values of θ_c obtained from velocity profiles at critical stage are shown below

Material	θ_c
Sand	0.0914
Walnut shell	0.0378
Coal	0.0436

The relationship between the mean velocity $\bar{V}$ and the shear velocity V_* for the three bed materials are shown in Figure 2. The bedload transport rate in the flume tests were measured by taking samples from a pan trap. The quantity by weight of the sediment was determined after drying. On the average, three samples per run were taken. The mean sediment transport rates were considered to be the average of the three samples. The latter was assumed to represent the long-time average bedload transport prevailing in the flume. The results of sediment transport tested in the flume are shown in Figure 3.

A schematic plan view of the model basin is shown in Figure 4. The maximum still water depth in the constant depth portion was approximately 11 inches. The channel connecting the two basin was 10.75 feet long and 2.75 feet wide. The beach was arranged to have a 1:20 slope (i.e., $\tan\alpha = 0.05$). The velocity profile in the channel was measured by the propeller-type velocity meter at different depths. The mean velocity was then taken by averaging the velocities over the full water depth. The three types of sediment materials used in the flume were also used in the model basin study. The water depth for each material was selected to satisfy the similarity laws. Waves were generated by a flap-type wave generator with variable periods and wave heights. The waves were made to approach the shore at an angle of ten degrees with respect to the normal of the shoreline. The flood and ebb flows were controlled by weir boxes and gates. The bedload transport rates in the model on the ocean side were measured by taking samples from a pan trap located under the sand weir.

TABLE 1

Test conditions in the model basin

Conditions	Sand	Walnut Shell	Coal
Depth in the channel (in.)	5.25	5.62	4.06
Depth in the ocean (in.)	8.125	8.57	7.72
Velocity in the channel (ft/sec.)			
Flood	0.646	0.665	0.568
Ebb	0.675	0.724	0.598
Wave period (sec.)	0.859	0.875	0.729
Wave height (ft.)	0.093	0.102	0.073
Test duration* (min.)	180	29	85

*The test duration was determined experimentally as the duration for accumulating equal volumes of bed material in the weir trap.

The results of longshore bedload transport is shown in Figure 5. After the completion of each test, the bottom configurations were contoured and recorded photographically. Three bottom section profiles, based on photographic records, are shown in Figure 6 through Figure 8 for the analysis.

DISCUSSION

The results of the velocity profiles measured in the flume tests were used to determine the dimensionless shear stress coefficients θ_c. The value of θ_c for sand in this study is approximate the same as that shown by Bagnold in his study (9). The grain size used in his study was 0.31 mm, and the θ_c was found at the range of values from 0.05 to 0.14. According to Bagnold, θ_c is a function of static volume concentration and the internal friction angle of bed material. The magnitude of θ_c does affect the intensity of the movement of bed material.

The linear relationship between the mean velocities and shear velocities are shown for the purpose of selecting the constant friction coefficients. The results of the velocity measurements were taken both in plane and dune beds. The reason for selecting the friction coefficient as constant is that the test velocity was scaled to a little higher than the velocity for bedload movement in the critical condition. The error introduced cannot be very significant as a linear velocity distribution in the boundary layer was assumed.

Figure 3 is a graphical comparison of the results by using Einstein's bedload function theory. The data for coarse bed materials fit Einstein's bedload function very well. The experimental results by Bishop, Simons and Richardson (10) showed that A_* and B_* are not universal constants but are related to the median diameter of the bed material. The results of the present study showed that the values of A_* increase with increasing grain size, and the values of B_* decrease with increasing grain size and that A_* and B_* are independent of the types of bed material. These characteristics of A_* and B_* are similar to the results shown by Bishop *et al*.

For the tests in the model basin, it is assumed that the bedload transport due to combined action of waves and currents is a function of bottom shear stress. Since the movement of

bedload due to wave action is related to the probability characteristics, the theory of Einstein's bedload function can be assumed to be valid in this study provided the dependence of the bottom shear stress on the oscillatory mean flows is taken into account. The equations of combined shear stresses were derived for this purpose. However, these derivations were based on the assumption that the velocity profile, from the edge of the viscous sublayer to the granular surface, is linear. Some discrepancy may occur for low water velocity. The error introduced by this can be reduced due to the effect of oscillating bottom water particle velocity, and the error is usually insignificant (11).

The velocity of longshore current was introduced according to Eagleson's formula. The derivation of Eagleson's formula was based on the conservation of momentum transported parallel to the shoreline. In the vicinity of an inlet, a similar analysis of momentum normal to the shoreline may be made and is seen to give a net flux of momentum into the inlet. The latter may be interpreted in terms of net velocity into the inlet in analogy to the longshore current in Eagleson's analysis. Consequently, the value of bottom shear stress should be higher than the one calculated by equation of flood flow inside inlet channel.

The coefficient p_1 of horizontal orbital velocity above the viscous sublayer was determined experimently in this study. The value of p_1 was determined from the duration of a test to accumulate a predetermined volume of sediment. From Figure 5, the shear stress was estimated, and using the combined shear stress equation, p_1 was evaluated. Using the three different bedload materials, three values of p_1 were obtained for three test durations which corresponded to the same volume transport rate. The final value of p_1 was evaluated according to results that have the best fit both in sediment transport rate and sedimentological time as compared with the estimated curves and the test durations. The value of p_1, in this atudy, was found to be 0.24. Bijker (11) derived the value of p_1 on the basis of Prandtl's shear stress equation and p_1 was found to be a constant value of 0.39. His experimental result of p_1, however, was 0.48. The reason his experimental result of p_1 was higher than the one found in this study may be due to many sand traps introduced during the test. Too many sand traps introduced during

the test may chang the bottom roughness and increase the value of p_1.

The bedload transport rate in the inlet was not directly. However, the bottom configurations were recorded photographically. It is possible to analyze the variation of bottom configurations by using those photographs. Three bottom section profiles in tne vicinity of inlet are shown in Figure 6 through Figure 8 for the analysis. Generally speaking, the results of hydrographical variation at the same location are similar to each other for flood and ebb flow with waves but exibit a difference for coal under the action of waves only. Although a complete justification for this difference is not know, the existence of a small current may interact the waves to produce a significant difference in shear stress.

Based on Newton's second law, Eagleson, Glenne and Dracup derived the equilibrium conditions for a stable beach (12). It is important to consider this equilibrium condition if one tries to obtain reasonable results. According to this equilibrium condition, there is no bedload movement in the direction normal to the beach under the action of a certain value of wave height. If the wave height is higher than this value, the beach slope changes. In this study, all the tests with coal, walnut shell,and sand had this consideration. The final results concerning the longshore sediment transport appeared satisfactory with the estimated curves.

CONCLUSIONS

From the basic study of bedload movement and the test results, the parameters involved in the modeling of sediment transport oan be expressed as the function of Froude number, bottom shear stress, friction factor, and wave steepness. The parameters, so selected, give better corelation for various movement of bedload in the ooastal environment. The dimensionless bedlaod intensity ϕ' was obtained aocording to the theory of Einstein's bedload function $\phi' = f(\psi')$. The dimensionless shear intensity ψ', however, was determined from the combined shear stresses due to the waves and currents. The results of longshore sediment transport rate were favorable compared with the estimated values for each bed material. However, they were not in close agreement for the tests of walnut shell and sand under the combined action due to waves and ebb flow.

In this study, the values of friction coefficient C_Z for each bed material were obtained with reasonable accuracy in the flume test. However, if the friction coefficient C_Z in the prototype cannot be well estimated, the results obtained in the model test will be influenced. Since it is always difficult to predict these values with sufficient accuracy, computation of the scale factor will have to be performed with different values of C_Z. From these computations, the possible variation in the scale factors, resulting from a wrong evaluation of the friction, can then be predicted.

For sediment transport research, most people are interested in knowing how accurate the sediment time scales are by introducing a weir trap in the model basin. The results show that the predicted sedimentological time ran 31 per cent less than the test durations for walnut shell and 36 per cent for coal. The scaled sedimentological time for each bed material will affect the changes in bottom configuration. If the considered parameters were perfect in scale, the bottom configuration should result in the same scaled topography during the test of the scaled sedimentological time. The results of the bottom configuration in this study are similar to each other except for the wave test on coal.

Although certain difficulties remain for predicting the sedimentological time scale, owing to the inadequate knowledge of flow near rough boundaries, the equation shown in this study is still useful in estimating test duration in model studies.

ACKNOWLEDGMENTS

This is a condensed report from a master thesis originally presented to the Graduate Council of the University of Florida, in August 1969.

The author is indebted to Dr. O. H. Shemdin and Dr. R. G. Dean for valuable guidance, suggestions and critical reading of the master thesis. The author also wishes to express his gratitude to Dr. B. A. Christensen for his review of the analytical results and for his constructive suggestions.

APPENDIX I

INTEGRATION OF BED SHEAR STRESSES DUE TO THE COMBINED ACTION OF WAVES AND CURRENTS

Equation (8) through Equation (11) can be integrated for one wave period by the following considerations.

Ebb flow inside channel

$$\text{If } \left(1 - \xi \frac{p_1 u_o}{V_m}\cos\theta\right) \geq 0,$$

$$\tau = \frac{1}{T}\int_0^T \tau(t)\,dt = \frac{1}{T}\rho V_{m_*}^2 \left[1 + \frac{1}{2}\left(\xi \frac{p_1 u_o}{V_m}\cos\theta\right)^2\right] \qquad \text{(I-1}$$

$$\text{If } \left(1 - \xi \frac{p_1 u_o}{V_m}\cos\theta\right) < 0,$$

$$\tau = \frac{1}{T}\int_0^T \tau(t)\,dt = \frac{1}{T}\rho V_{m_*}^2 \left[1 + \frac{1}{2}\left(\xi \frac{p_1 u_o}{V_m}\cos\theta\right)^2 - 2\int_{t_1}^{t_2} \left(1 - \xi \frac{p_1 u_o}{V_m}\cos\theta \sin\sigma t\right)^2 dt\right] \qquad \text{(I-2}$$

where $t_1 = \frac{1}{\sigma}\sin^{-1}\left(\frac{V_m}{\xi p_1 u_o \cos\theta}\right)$ $\qquad t_2 = \pi - t_1$

Simplifying Equation (I-2), it follows that

$$\tau = \frac{1}{T}\int_0^T \tau(t)\,dt = \frac{1}{T}\rho V_{m_*}^2 \left\{\left[1 + \frac{1}{2}\left(\xi \frac{p_1 u_o}{V_m}\cos\theta\right)^2\right]\left[1 - (2\pi - 4t_1)\right] + \frac{8}{\sigma}\left(\xi \frac{p_1 u_o}{V_m}\cos\theta\right)\cos\sigma t_1\right\} \qquad \text{(I-3)}$$

Ebb flow parallel to the shoreline

$$\tau = \frac{1}{T}\int_0^T \tau(t)\,dt = \pm \frac{1}{T}\rho V_{L_*}^2 \left[\left(\frac{V_L - V_y}{V_L}\right)^2 + \frac{1}{2}\left(\xi \frac{p_1 u_o}{V_L}\sin\theta\right)^2\right] \qquad \text{(I-4)}$$

where

"+" sign for $\frac{V_L - V_y}{\xi p_1 u_o \sin\theta} \geq 1$

"-" sign for $\frac{V_L - V_y}{\xi p_1 u_o \sin\theta} \leq -1$

If $0 < \left(\frac{V_L - V_y}{\xi p_1 u_o \sin\theta}\right) < 1$ or $-1 < \left(\frac{V_L - V_y}{\xi p_1 u_o \sin\theta}\right) < 0$

$$\tau = \frac{1}{T}\int_0^T \tau(t)\, dt = \pm \frac{1}{T}\rho V_{L*}^2\left\{\left[\left(\frac{V_L - V_y}{V_L}\right)^2 + \frac{1}{2}\left(\xi \frac{p_1 u_o}{V_L}\sin\theta\right)^2\right]\right.$$
$$\left.\left[1 - (2\pi - 4t_1)\right] + \frac{8}{\sigma}\left(\xi \frac{p_1 u_o}{V_L}\sin\theta \cos\sigma t_1\right)\right\} \quad \text{(I-5)}$$

where

$$t_1 = \frac{1}{\sigma}\sin^{-1}\left(\frac{V_L}{\xi p_1 u_o \sin\theta}\right)$$

and

"+" sign for $0 < \frac{V_L - V_y}{\xi p_1 u_o \sin\theta} < 1$

"-" sign for $-1 < \frac{V_L - V_y}{\xi p_1 u_o \sin\theta} < 0$

If $\frac{V_L - V_y}{\xi p_1 u_o \sin\theta} = 0$

$$\tau = \frac{1}{T}\int_0^T \tau(t)\, dt = 0 \quad \text{(I-6)}$$

Flood flow inside channel

If $\frac{\frac{q_x}{q}}{\xi \frac{p_1 u_o}{q}\cos\theta} \geq 1$

$$\tau = \frac{1}{T}\int_0^T \tau(t)\, dt = \frac{1}{T}\rho q_*^2\left[\left(\frac{q_x}{q}\right)^2 + \frac{1}{2}\left(\xi \frac{p_1 u_o}{q}\cos\theta\right)^2\right] \quad \text{(I-7)}$$

If $0 < \dfrac{\frac{q_x}{q}}{\xi \frac{p_1 u_o}{q}\cos\theta} < 1$

$$\tau = \frac{1}{T}\int_0^T \tau(t)\,dt = \frac{1}{T}\rho q_*^2 \left\{ \left[\left(\frac{q_x}{q}\right)^2 + \frac{1}{2}\left(\xi \frac{p_1 u_o}{q}\cos\theta\right)^2 \right] \left[1 - (2\pi - 4t_1)\right] + \frac{8}{\sigma}\left(\xi \frac{p_1 u_o}{q}\cos\theta\right)\cos\sigma t_1 \right. \quad \text{(I-8)}$$

where

$$t_1 = \frac{1}{\sigma}\sin^{-1}\left(\frac{q}{\xi p_1 u_o \cos\theta}\right)$$

Flood flow parallel to the shoreline

$$\tau = \frac{1}{T}\int_0^T \tau(t)\,dt = \pm \frac{1}{T}\rho V_{L_*}^2 \left[\left(\frac{V_L - q_y}{V_L}\right)^2 + \frac{1}{2}\left(\xi \frac{p_1 u_o}{V_L}\sin\theta\right)^2 \right] \quad \text{(I-9)}$$

where

"+" sign for $\dfrac{V_L - q_y}{\xi p_1 u_o \sin\theta} \geq 1$

"-" sign for $\dfrac{V_L - q_y}{\xi p_1 u_o \sin\theta} \leq -1$

If $0 < \dfrac{V_L - q_y}{\xi p_1 u_o \sin\theta} < 1$ or $-1 < \dfrac{V_L - q_y}{\xi p_1 u_o \sin\theta} < 0$

$$\tau = \frac{1}{T}\int_0^T \tau(t)\,dt = \pm \frac{1}{T}\rho V_{L_*}^2 \left\{ \left[\left(\frac{V_L - q_y}{V_L}\right)^2 + \frac{1}{2}\left(\xi \frac{p_1 u_o}{V_L}\sin\theta\right)^2 \right] \left[1 - (2\pi - 4t_1)\right] + \frac{8}{\sigma}\left(\xi \frac{p_1 u_o}{V_L}\sin\theta\right)\cos\sigma t_1 \right\} \quad \text{(I-10)}$$

where

$$t_1 = \frac{1}{\sigma}\sin^{-1}\left(\frac{V_L}{\xi p_1 u_o \sin\theta}\right)$$

and

$$\text{"+" sign for } 0 < \frac{V_L - q_y}{\xi p_1 u_o \sin\theta} < 1$$

$$\text{"-" sign for } -1 < \frac{V_L - q_y}{\xi p_1 u_o \sin\theta} < 0$$

If $\frac{V_L - q_y}{V_L} = 0$

$$\tau = \frac{1}{T}\int_0^T \tau(t)\, dt = 0 \qquad \text{(I-11)}$$

NOTATIONS

A_*, B_*	Constants determined experimentally
B_1	Channel width
C_z	Chēzy's coefficient
C_o	Static volume concentration of bed material
C_2	Empirical constant
d	Water depth in the channel
d_b	Water depth at breaker
d_e	Grain size of bedload which is 50 per cent finer by weight
F_o	Dimensionless parameter
f	Darcy-Weisbach's coefficient
g	Gravity acceleration
H	Wave height
H_b	Wave height at breaker
k	Wave number
k_e	Roughness height
L	Wave length
n_b	Ratio of group velocity with respect to wave celerity at breaker
p	Porosity of bed material
p_1	Coefficient of horizontal orbital velocity above the laminar sublayer
Q	Rate of water discharge

q	Velocity in potential flow field
q_s	Volume discharge of sediment transport per unit time per unit width
q_w	Weight discharge of sediment transport per unit width
q_x	Velocity component of q in x-direction
q_y	Velocity component of q in y-direction
q_*	Shear velocity in potential flow
S_f	Specific gravity of water
S_s	Specific gravity of bedload
u	Orbital velocity in x-dircetion
u_b	Orbital velocity at bottom
V_L	Longshore velocity
V_m	Velocity in the approach flow
V_x	Velocity in the region of channel expansion
V_*	Shear velocity
V_{m_*}	Shear velocity in the approach flow
V_{x_*}	Shear velocity in the region of channel expansion
α	Beach slope angle
α_i	Internal friction angle
κ	Von Karman's universal constant
θ	Angle that the velocity vector in potential flow makes with the positive x-axis
ϕ	Velocity potential
ψ	Stream function

REFERENCES

1. Einstein, H. A. The Bed Load Function for Sediment Transportation in Open Channel Flow, U.S. Dept. of Agr., Tech. Bull. No. 1026, 1950.

2. Kalkanis, G. Transportation of Bed Material Due to Wave Action. U.S. Army Corps of Engr., Tech. Memo. No. 2, 1964.

3. Tollmien, W. Momentum Transfer Theory for a Jet, Translation, Tech. Memo. 1085, NACA (currently, NASA), Washington, D.C., 1945; originally in Z.A.A.M., Vol. 6, pp. 468-475, 1926.

4. Albertson, M. L., Dai, Y. B., Jensen, R. A., and Rouse, Hunter, Diffusion of Submerged Jets, Proceedings, ASCE, Vol. 74, No. 10, pp. 1157-1196, 1948.

5. Baines, W. Douglas, Discussion of "Diffusion of Submerged Jets" by M. L. Albertson, Y. B. Dai, R. A. Jensen, and Hunter Rouse, Transactions, ASCE, Vol. 115, pp. 677-684, 1950.

6. French, J. L. Tidal Flow in Entrances, U.S. Army Corps of Engrs. Tech. Bull. No. 3, 1960.

7. Eagleson, P. S. Theoretical Study of Longshore Currents on a Plane Beach, M.I.T. Hydrodynamics Lab., Rep. No. 82, 1965.

8. Bagnold, R. A. An Approach to the Sediment Transport Problem from General Physics, Geological Survey, Prof. Paper 422-I, 1966.

9. Bagnold, R. A. Flow of Cohesionless Grains in Fluids, Philo. Trans. of Royal Soc., Vol. 249, pp. 235-197, 1956.

10. Bishop, A. A., Simons, D. B., and Richardson, E. V. Total Bed Material Transport, Journal of Hydr. Div., ASCE, Vol. 91, No. HY2, March, 1965.

11. Bijker, E. W. Some Considerations about Scales for Coastal Model with Movable Bed, Delft Hydr. Lab. Report, Publ. No. 50, 1967

12. Eagleson, P. S., Glenne, B., and Dracup, J. A. Equilibrium Characteristics of Sand Beaches, Journal of Hydr. Div., ASCE, Paper No. 3387, pp. 35-37, January, 1963.

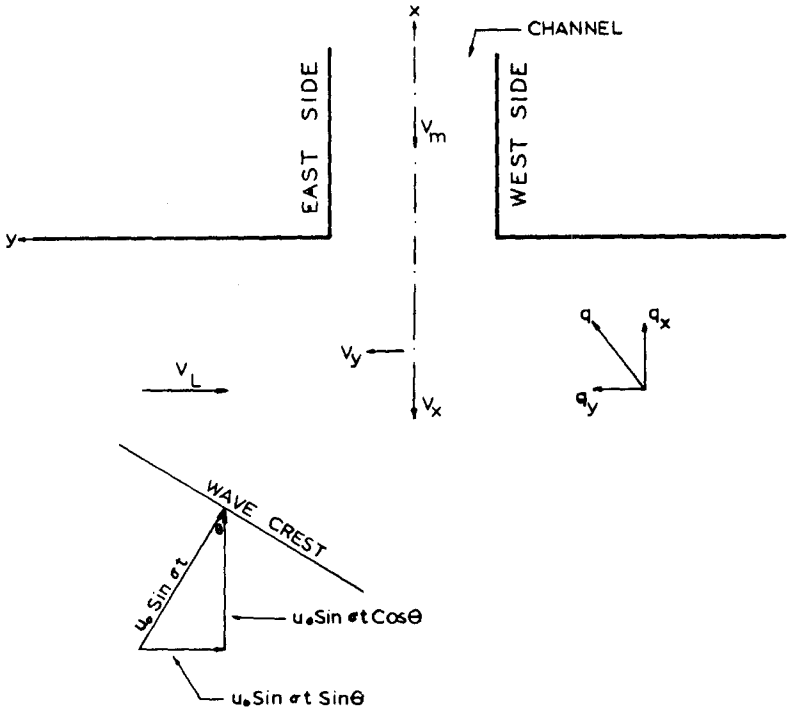

Fig. I_a General representation of currents and waves

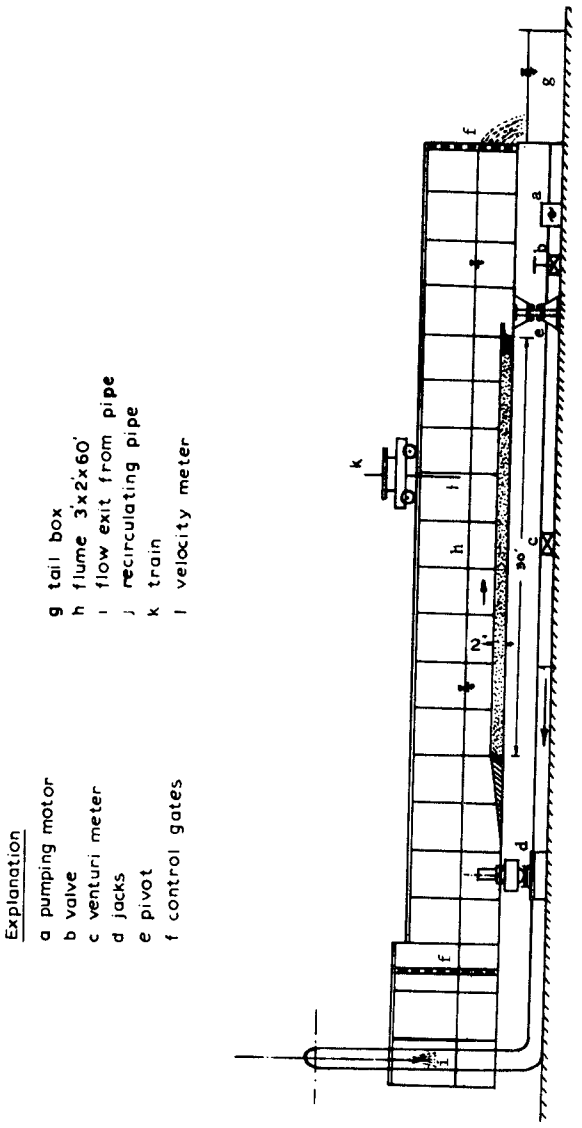

Fig. 1b Schematic diagram of the flume

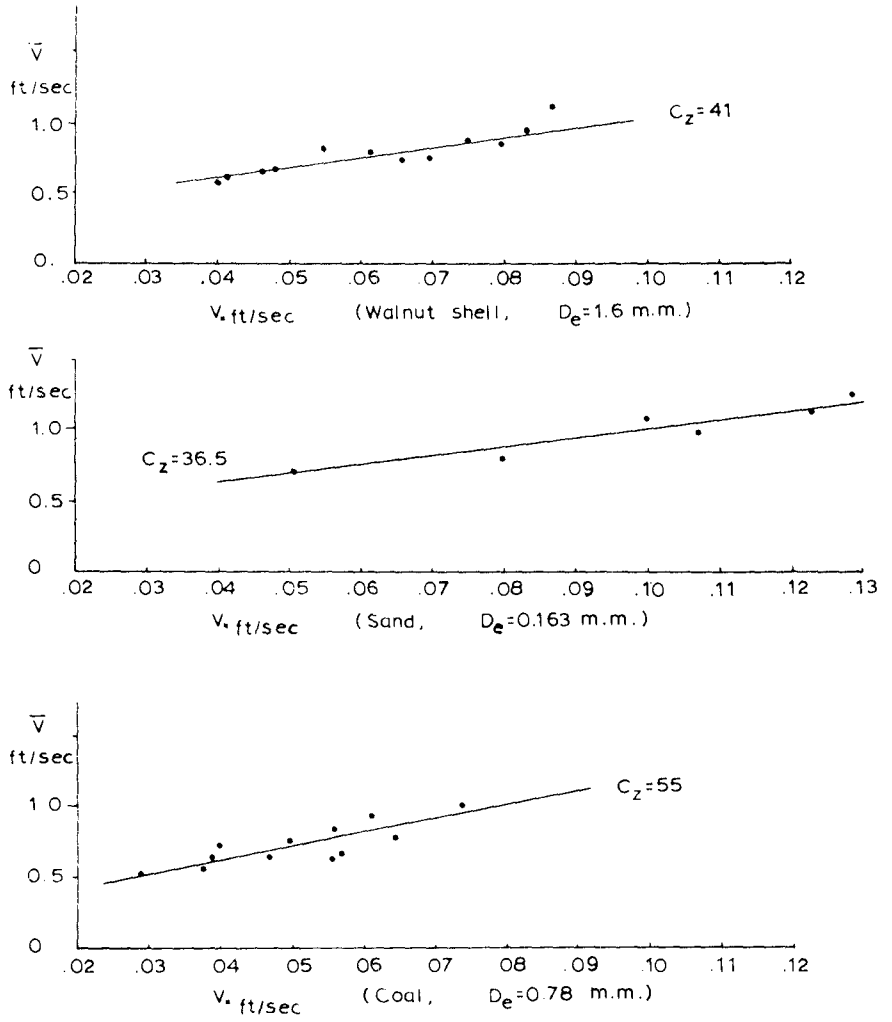

Fig 2 $\bar{V}$ vs. V_* for plane and dune beds

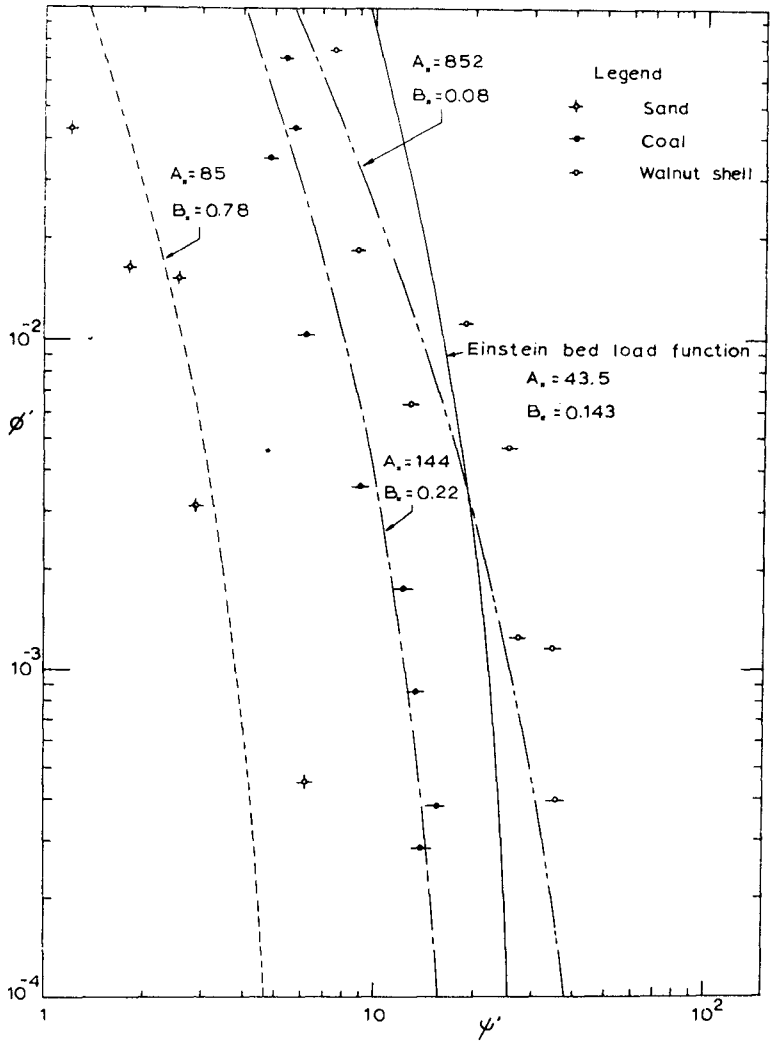

Fig. 3 ϕ'-ψ' curves for the three different bed materials tested in the flume

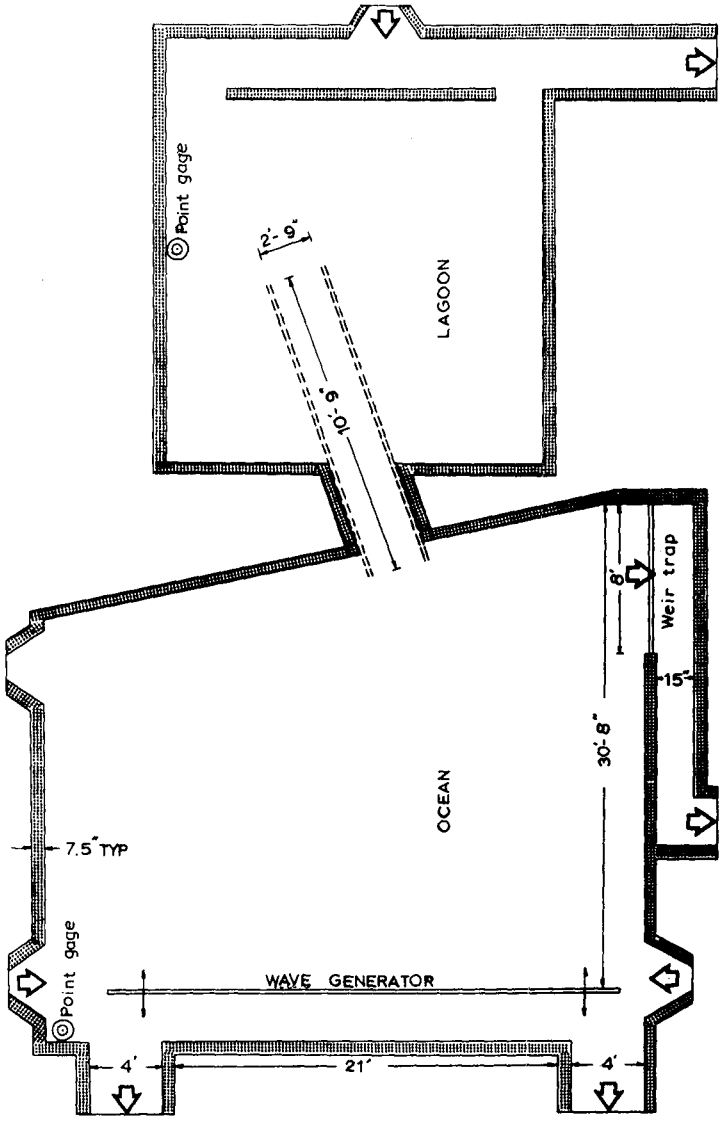

Fig. 4 Schematic diagram of model basin

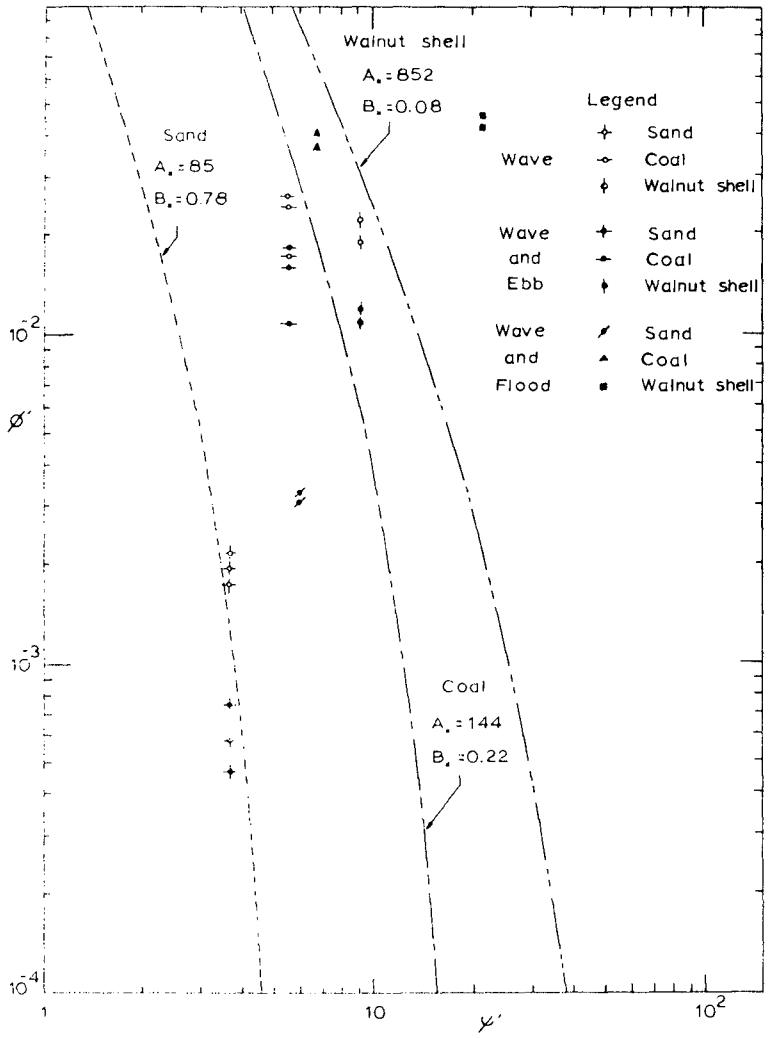

Fig. 5 The tested results in the model basin as compared with the estimated ϕ'- ψ' curves

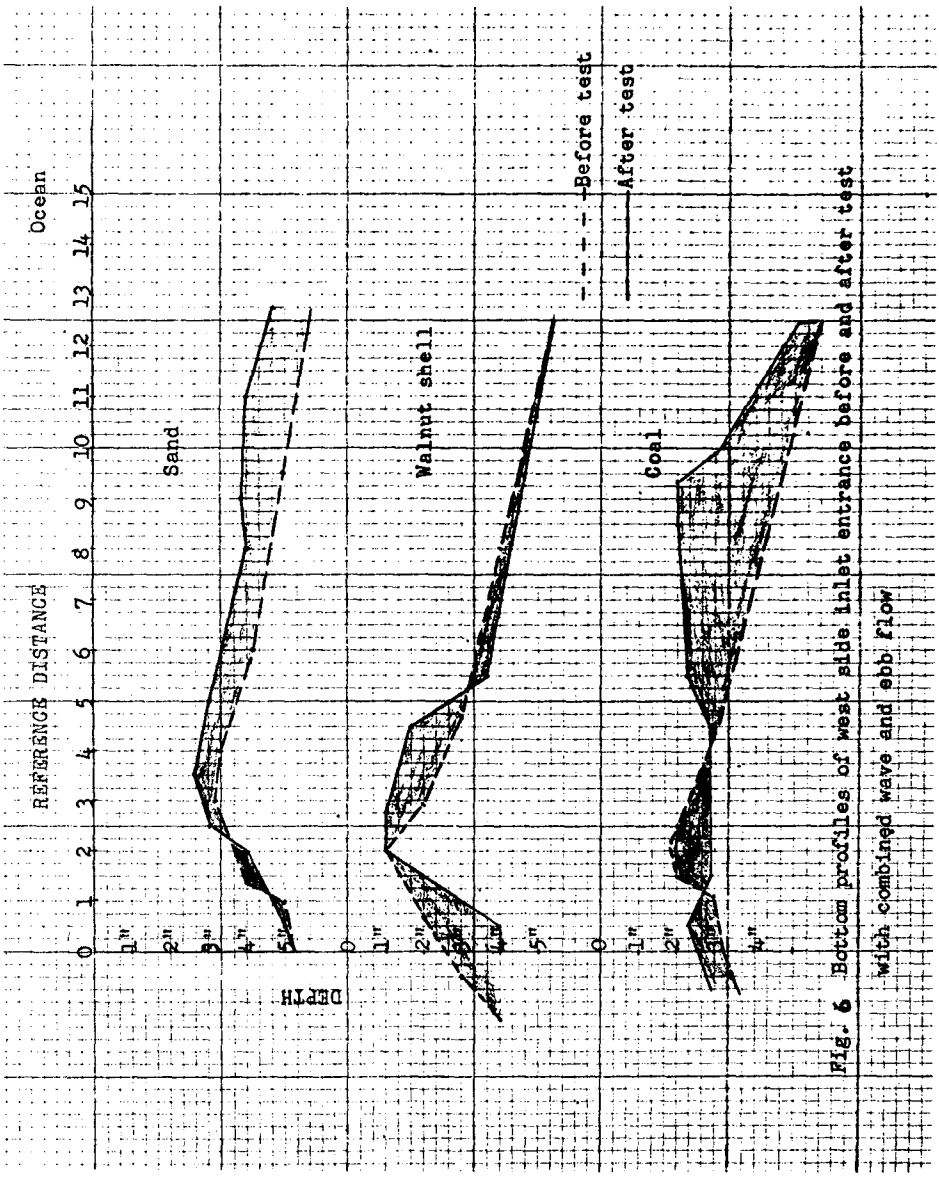

Fig. 6 Bottom profiles of west side inlet entrance before and after test with combined wave and ebb flow

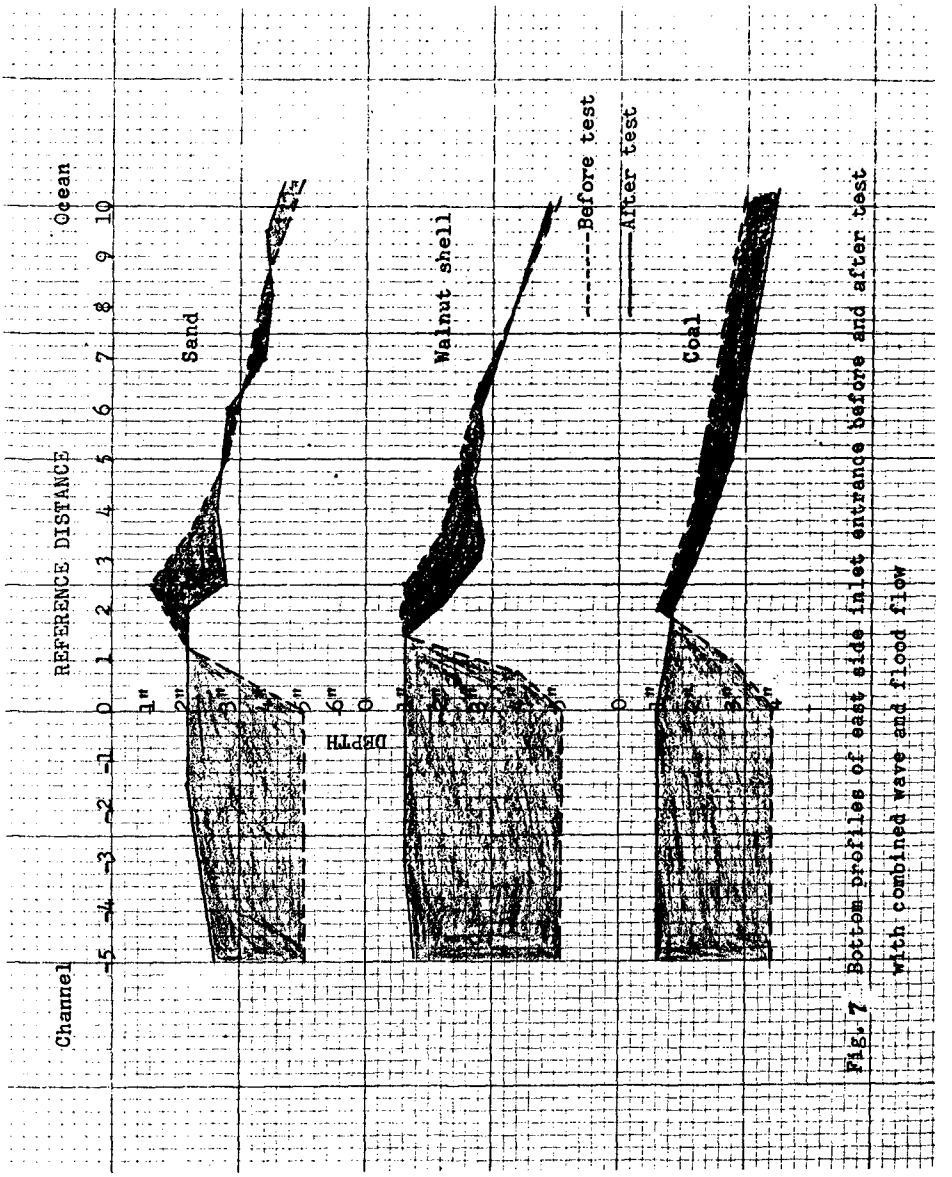

Fig. 7 Bottom profiles of east side inlet entrance before and after test with combined wave and flood flow

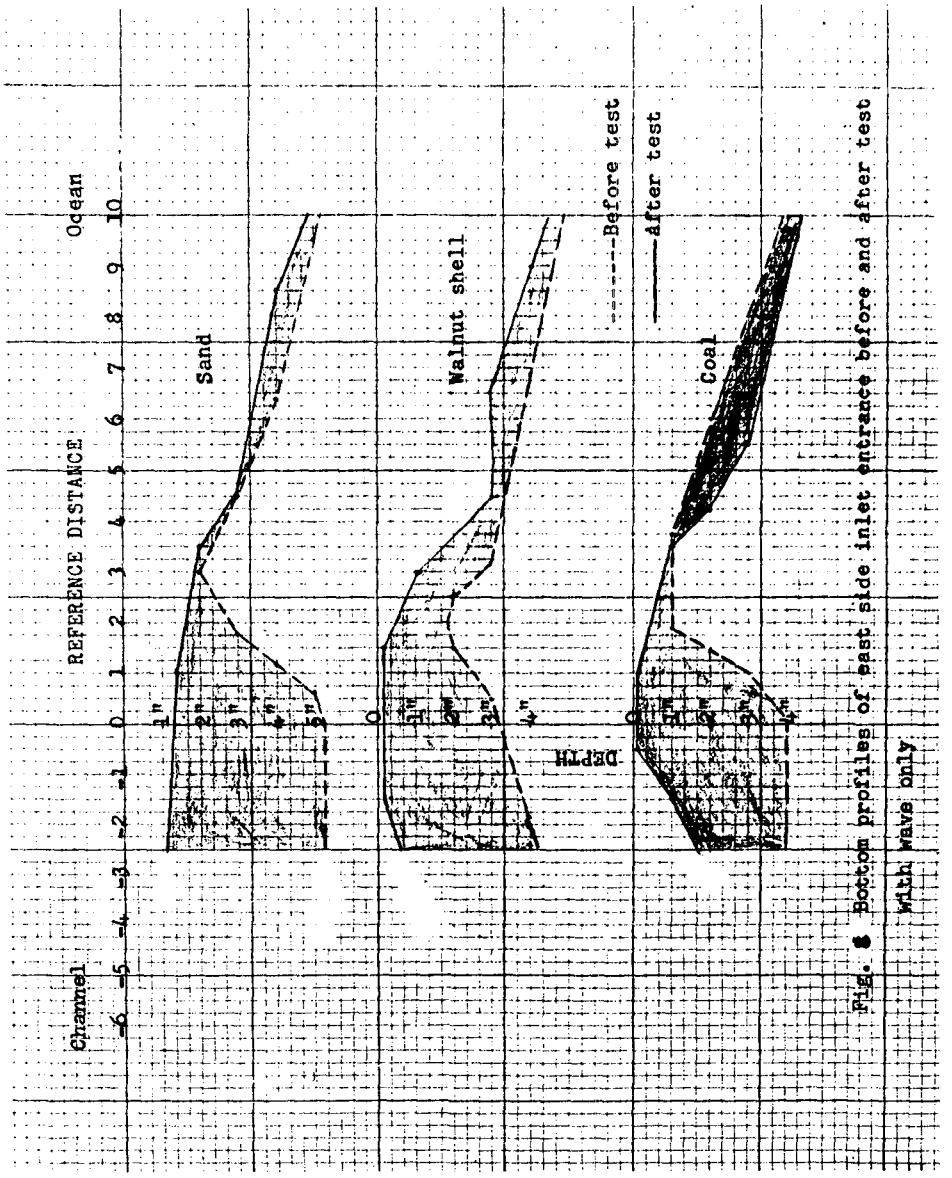

Fig. 8 Bottom profiles of east side inlet entrance before and after test with wave only